Electron-impact triple ionization of Se^{2+}

Jurgita Koncevičiūtė, Sigitas Kučas, Šarūnas Masys, Aušra Kynienė, and Valdas Jonauskas*
Institute of Theoretical Physics and Astronomy, Vilnius University, Saulėtekio av. 3, LT-10257 Vilnius, Lithuania

(Received 3 November 2017; published 22 January 2018)

It is shown that triple ionization (TI) of the Se^{2+} ion is mainly formed in two ways: (i) Auger cascade following single ionization of the $3p$ shell and (ii) direct double ionization (DDI) with subsequent autoionization. A good agreement with recent experimental measurements is obtained when one of electrons in the DDI process acquires all the excess energy. The study also reveals negligible contribution of the direct TI by electron impact to the process. Single-ionization cross sections of the excitation-autoionization process show large dependence on the levels of the ground configuration. The obtained results demonstrate that the ions in the parent beam mainly reside in the highest level of the ground configuration.

DOI: 10.1103/PhysRevA.97.012705

I. INTRODUCTION

Electron-impact single and multiple ionization processes are of both fundamental and applied interests, since they provide an understanding of the electronic dynamics and the structure of the target. Electron-impact ionization processes have a wide range of applicability that varies from plasma physics [1], stellar atmospheres [2,3], to cancer treatment by irradiation [4–6].

Selenium has been detected in various astrophysical nebulae and metal-poor stars [7–12]. This element is potentially useful in studies for nucleosynthetic models of stellar populations. These studies require accurate atomic data for processes such as photoionization, autoionization, dielectronic recombination, as well as electron-impact excitation and ionization.

Single-, double-, and triple-ionization cross-section measurements for the Se^{2+} ions from their ionization thresholds up to 500 eV [13] and for the Se^{3+} ions from their ionization thresholds up to 1 keV [14] were carried out at the Multicharged Ion Research Facility of the University of Nevada in Reno using the dynamic-crossed-beams technique [15]. The experimental values were compared with data calculated from the Lotz semiempirical formula for the direct ionization [16]. The observed differences suggested large contribution from the indirect process. In addition, a semiempirical formula for double ionization (DI) [17] was used to obtain a least-squares fit of the experimental data.

Recently, the semirelativistic configuration-average distorted-wave (CADW) method was applied to calculate electron-impact single- and double-ionization cross sections for the Se^{2+} and Se^{3+} ions [18]. Direct and indirect processes were investigated for the ground configurations of the ions. To our knowledge, at the moment, no *ab initio* studies are available for triple-ionization (TI) process of both the Se^{2+} and Se^{3+} ions.

In this paper, we aim to study electron-impact TI process of the Se^{2+} ion by considering (i) Auger cascade following creation of the inner shell vacancy, and (ii) the direct double-ionization (DDI) process with subsequent autoionization. The DDI process using a few-step approach was investigated for the O^+, O^{2+}, O^{3+}, C^{1+}, Ar^{2+}, and Li^{1+} ions and a good agreement with measurements was established [19,20]. A few-step approach applied for the DDI process involves ionization-ionization (II), excitation-ionization-ionization (EII), and ionization-excitation-ionization (IEI) paths. Therefore, the study of single- and double-ionization cross sections is also presented and compared with experimental data [13].

The rest of the paper is organized as follows. In Sec. II, an overview of the theoretical approach used to calculate single-, double-, and triple-ionization cross sections is given; single-, double-, and triple-ionization cross sections for the Se^{2+} ion are presented and compared with experimental measurements in Sec. III; a brief summary with some final conclusions and directions for future work are provided in Sec. IV.

II. THEORETICAL APPROACH

Electron-impact single ionization (SI) can occur via direct and indirect processes. The total SI cross sections from the level i of the initial ion to the level f of the ionized ion can be expressed by the equation:

$$\sigma_{if}^{\mathrm{SI}}(\varepsilon) = \sigma_{if}^{\mathrm{CI}}(\varepsilon) + \sum_j \sigma_{ij}^{\mathrm{CE}}(\varepsilon) B_{jf}. \tag{1}$$

Here, $\sigma_{if}^{\mathrm{CI}}(\varepsilon)$ is the cross section of the direct single collisional ionization (CI) process, ε is the energy of the incident electron, $\sigma_{ij}^{\mathrm{CE}}(\varepsilon)$ is the electron-impact excitation cross section to the intermediate level j of the initial ion, and B_{jf} is the branching ratio for the autoionization process from the level j to the final level f. The second term describes the indirect process: excitation autoionization (EA). The autoionization branching ratio can be expressed as

$$B_{jf} = \frac{A_{jf}^a}{\sum_m A_{jm}^a + \sum_n A_{jn}^r}, \tag{2}$$

*Valdas.Jonauskas@tfai.vu.lt

where A^a and A^r are the Auger and radiative transition probabilities, respectively.

In the case of DI, again, direct and indirect processes are possible. Equation for the total DI cross sections from the level i of the initial ion to the level f of the doubly ionized ion can be expressed as a sum of direct and indirect processes:

$$\sigma_{if}^{\mathrm{DI}}(\varepsilon) = \sigma_{if}^{\mathrm{DDI}}(\varepsilon) + \sum_j \sigma_{ij}^{\mathrm{CI}}(\varepsilon) B_{jf}, \tag{3}$$

where $\sigma_{if}^{\mathrm{DDI}}$ is the DDI cross sections and a term $\sum_j \sigma_{ij}^{\mathrm{CI}}(\varepsilon) B_{jf}$ describes the indirect double-ionization process: ionization with autoionization (IA) through the intermediate level j of the ionized ion.

Electron-impact DDI cross sections for the Se^{2+} ion are studied using previously proposed two- and three-step approaches [19], that describe DDI by the II, IEI, and EII processes.

Thus, the equation for the DDI process from the level i to the level f through the II path can be written as

$$\sigma_{if}^{\mathrm{DDI(II)}}(\varepsilon) = \sum_j \sigma_{ij}^{\mathrm{CI}}(\varepsilon) \frac{\sigma_{jf}^{\mathrm{CI}}(\varepsilon_1)}{4\pi \bar{R}_{nl}^2}, \tag{4}$$

here ε_1 is the energy of the scattered or ejected electron, which in the further step collides with one of the remaining bound electrons from the nl shell and knocks it off. Factor $\frac{\sigma_{jf}^{\mathrm{CI}}(\varepsilon_1)}{4\pi \bar{R}_{nl}^2}$ determines the probability of the second electron-impact ionization process under assumption that the density of the electrons in the shell is uniform, $\bar{R}_{nl}$ is the mean distance of the electrons from the nucleus. $\sigma_{jf}^{\mathrm{CI}}(\varepsilon_1)$ is the electron-impact direct SI cross sections from the intermediate level j to the final level f.

Another possible path for DDI, the EII process, can be expressed by the equation

$$\sigma_{if}^{\mathrm{DDI(EII)}}(\varepsilon) = \sum_{kj} \sigma_{ik}^{CE}(\varepsilon) \frac{\sigma_{kj}^{\mathrm{CI}}(\varepsilon_1)}{4\pi \bar{R}_{nl}^2} \frac{\sigma_{jf}^{\mathrm{CI}}(\varepsilon_2)}{4\pi \bar{R}_{n'l'}^2}, \tag{5}$$

where $\varepsilon_1 = \varepsilon - \Delta E_{ik}$, ΔE_{ik} is a transition energy and ε_2 is the energy of the scattered or ejected electron.

Likewise, the DDI cross sections for the IEI process can be written as

$$\sigma_{if}^{\mathrm{DDI(IEI)}}(\varepsilon) = \sum_{kj} \sigma_{ik}^{\mathrm{CI}}(\varepsilon) \frac{\sigma_{kj}^{CE}(\varepsilon_1)}{4\pi \bar{R}_{nl}^2} \frac{\sigma_{jf}^{\mathrm{CI}}(\varepsilon_2)}{4\pi \bar{R}_{n'l'}^2}, \tag{6}$$

here $\frac{\sigma_{kj}^{CE}(\varepsilon_1)}{4\pi \bar{R}_{nl}^2}$ is the excitation probability of the electron from the nl shell of the level k to the level j by the scattered or ejected electron with energy ε_1.

Previously, it has been demonstrated that better agreement with measurements at the higher energies of the incident electron in the DDI process for the O^{1+}, O^{2+}, O^{3+}, C^{1+}, and Ar^{2+} ions [19] was obtained when it was assumed that the scattered and ejected electrons share the excess energy equally. On the other hand, mainly one of the electrons takes all the excess energy and participates in the further processes at the lower energies of the incident electron. In this work, both limiting cases of the energy distribution for the electrons have been investigated.

It is important to note that there are many studies devoted to analysis of final distribution of electron energies in the electron-impact DDI process. For example, double ionization of helium [21,22] provides unique opportunities to investigate a four-body Coulomb problem. The problem is simplified by considering fast incoming and scattered electron while energies of other two leaving electrons are relatively small. In our knock-out model, the energy of the electron participating in the next ionization or excitation process after being ionized has to be determined. Two limiting cases of energy distribution are studied in this work. Unfortunately, it is impossible to perform analysis of the final energies of the leaving electrons within our model framework.

Excited levels formed by the DDI process can decay further via autoionization (DDI-AI) to the next ionization stage. The additional step after DDI leads to TI. This process is possible if the energy of the excited level produced by the DDI process is higher than the TI threshold. Furthermore, contribution from Auger cascade when inner shell vacancy is formed by the incident electron has to be estimated. The Auger cascade is an important mechanism producing ions in the highly charged stages [23–26]. Therefore, electron-impact TI process is studied as a sum of the DDI-AI processes and Auger cascade following SI from the inner shell of the Se^{2+} ion.

Equations for the DDI process formed by the II, EII, and IEI paths with subsequent autoionization from the level i of the initial ion to the level f of the triply ionized ion can be written as

$$\sigma_{if}^{\mathrm{DDI(II)\text{-}AI}}(\varepsilon) = \sum_j \sigma_{ij}^{\mathrm{DDI(II)}}(\varepsilon) B_{jf}, \tag{7}$$

$$\sigma_{if}^{\mathrm{DDI(EII)\text{-}AI}}(\varepsilon) = \sum_j \sigma_{ij}^{\mathrm{DDI(EII)}}(\varepsilon) B_{jf}, \tag{8}$$

$$\sigma_{if}^{\mathrm{DDI(IEI)\text{-}AI}}(\varepsilon) = \sum_j \sigma_{ij}^{\mathrm{DDI(IEI)}}(\varepsilon) B_{jf}, \tag{9}$$

where DDI is described by the two- and three-step processes from the level i of the initial ion to the level j of the Se^{4+} ion [Eqs. (4), (5), and (6), respectively]. Autoionization process following DDI is represented in Eq. (7), (8), and (9) by the branching ratio B_{jf} from the level j of the Se^{4+} ion to the level f of Se^{5+}.

Energy levels, radiative and Auger transition probabilities, as well as electron-impact excitation and SI cross sections have been calculated using the flexible atomic code [27]. This code implements the Dirac-Fock-Slater approach. Single configuration approximation is used in this paper. Continuum orbitals of incident and scattered electrons are evaluated in the potential of the ionizing ion since this approach provides better agreement with experimental measurements. Electron-impact excitation and SI processes are investigated using the distorted-wave (DW) approximation.

III. RESULTS

Energy levels of the lowest configurations for the Se^{2+}, Se^{3+}, Se^{4+}, Se^{5+}, and Se^{6+} ions as well as single-, double-, and triple-ionization thresholds for the Se^{2+} ion are presented in Fig. 1. The SI threshold for the ground state of the Se^{2+} ion corresponds to 31.06 eV, which is in a good agreement

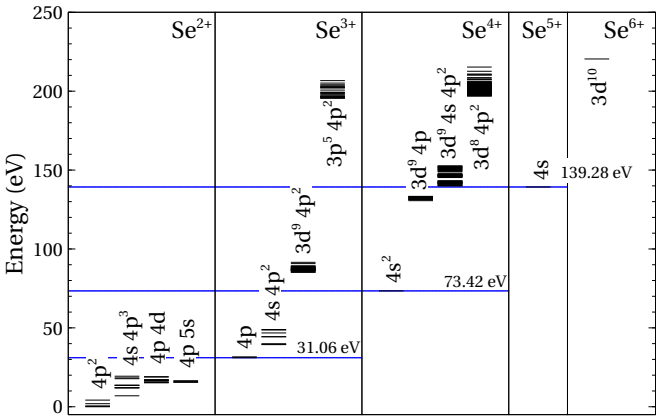

FIG. 1. Energy levels of the lowest configurations of the Se^{2+}, Se^{3+}, Se^{4+}, Se^{5+}, and Se^{6+} ions. Ionization thresholds are presented by horizontal lines with the corresponding values.

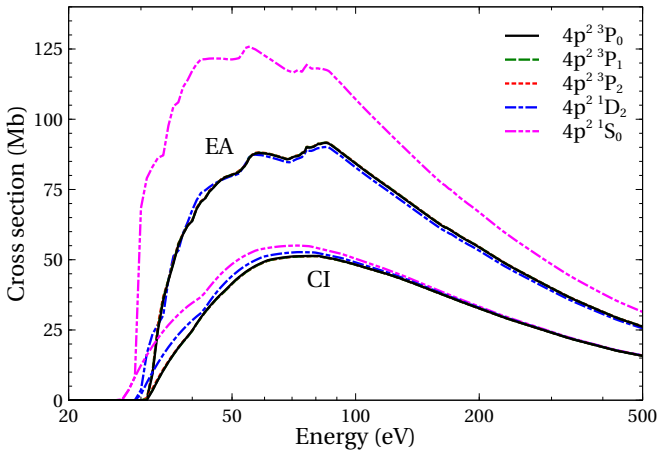

FIG. 2. Contributions of the CI and EA processes to SI of Se^{2+} for different energy levels of the ground configuration.

with the NIST value of 31.697 eV. Experimental cross sections start below the ground-state ionization threshold suggesting that metastable fraction is present in parent ion beam [13]. Our calculated energy levels of the Se^{2+} ground configuration together with the values from the NIST database [28] are presented in Table I. It can be seen that splitting of the theoretical energy levels of the ground configuration is higher than for the NIST data. This demonstrates the importance of correlation effects for the presented energy levels.

It can be seen from Fig. 1 that excited levels of the Se^{3+} ion corresponding to configuration with a vacancy in a $3d$ shell can decay to the Se^{4+} ion via Auger transitions since the energies of these levels are higher than the DI threshold of the Se^{2+} ion. In addition, the energies of the excited levels of the Se^{3+} ion corresponding to the configuration with a vacancy in a $3p$ shell are higher than the TI threshold of the Se^{2+} ion. Therefore, the Auger cascade may occur from this configuration leading to the transition to the Se^{5+} ion. Previous studies for the Kr ions demonstrated importance of the correlation effects for the Auger cascades [24–26]. Unfortunately, these calculations are very time consuming and have not been considered in this paper.

Analysis of contributions to the SI process (Fig. 2) from different levels of the ground configuration of the Se^{2+} ion shows slightly larger DI cross sections for the highest $4p^2\,{}^1S_0$ level (Table I). However, the EA process for this level demonstrates significant increase of the cross sections over entire range of energies, thus, providing much better agreement with experimental results compared to the contribution of other states of the ground configuration. Therefore, the single-, double-, and triple-ionization cross sections of the Se^{2+} ion are investigated for the $4p^2\,{}^1S_0$ level.

The total cross sections of SI by electron-impact for the Se^{2+} $4p^2\,{}^1S_0$ level are compared with experiment in Fig. 3. It has to be noted that influence of radiative damping is very small. Total SI cross sections are in a good agreement with experiment across the entire energy range of the incident electron. The largest contribution to the total cross sections comes from the excitations to configurations of the Se^{2+} ion with subsequent autoionization to the Se^{3+} ion. The contribution of direct ionization from the $4p$ shell is significantly larger than that of the $4s$ shell. The SI cross sections obtained in the potential of the ionized ion are lower by about 20% at the peak compared to the results presented here. This leads to the data below the experimental error bars for the highest values.

TABLE I. Energy levels of the ground (Ar) $3d^{10}4s^24p^2$ configuration of Se^{2+}. The NIST recommended values are presented for comparison.

Index	Term	J	Energy (eV)	NIST Energy (eV)
0	^3P	0	0.0000	0.000
1	^3P	1	0.2208	0.2159
2	^3P	2	0.5202	0.4881
3	^1D	2	1.9357	1.6158
4	^1S	0	4.2036	3.5249

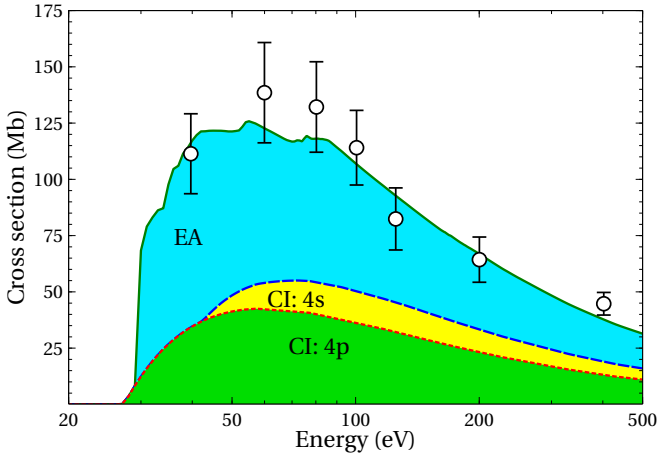

FIG. 3. Electron-impact SI of Se^{2+} for the $4p^2\,{}^1S_0$ level. Short-dashed line (red): CI of $4p$ shell; long-dashed line (blue): CI of $4p$ and $4s$ shells; solid line (green): CI with EA; empty circles: experiment [13]. Calculated contributions of the CI and EA processes are represented by the differently shaded (colored) areas.

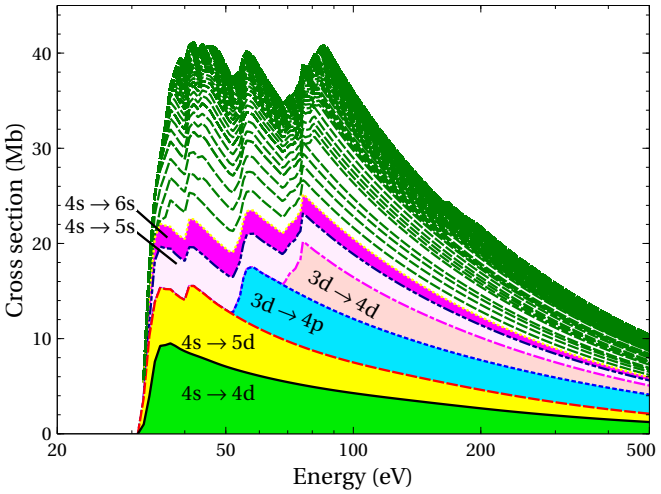

FIG. 4. Contributions of various EA channels to the total EA cross sections for the ground $4p^2\,{}^3P_0$ level. The strongest EA channels are represented by the differently shaded (colored) areas.

The strongest contributions to the EA process arise from the $4s \to 4d$, $4s \to 5d$, $3d \to 4p$, $3d \to 4d$, $4s \to 5s$, and $4s \to 6s$ excitations for the ground level (Fig. 4). Separate contribution of other excitations is much smaller. Surprisingly, the cross sections for the different EA channels drastically change for the excited $4p^2\,{}^1S_0$ level (Fig. 5). First of all, the contribution from the $4s \to 4d$ excitation increases about by a factor of four compared to excitation from the ground level. This amounts to about 35% at the peak of the EA cross sections. Second, the next strongest contributions correspond to the $4s \to 5s$, $4s \to 5p$, $4s \to 5d$, $3d \to 4p$, and $4s \to 4d$ excitations, which are presented in decreasing order of the strength. Furthermore, these excitations produce much larger contribution to the EA cross sections compared to excitation from the ground level. The observed differences can be explained by the fact that $4s\,4p^2\,4d$, $4s\,4p^2\,5s$, and $4s\,4p^2\,5p$ configurations straddle the single-ionization threshold. The

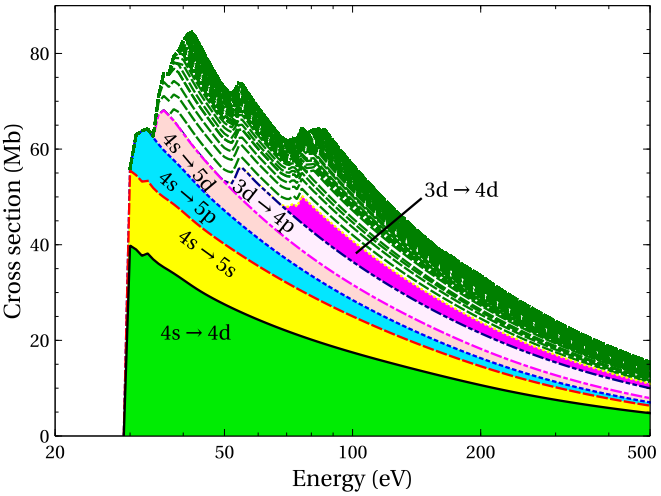

FIG. 5. Contributions of various EA channels to the total EA cross sections for the $4p^2\,{}^1S_0$ level. The strongest EA channels are represented by the differently shaded (colored) areas.

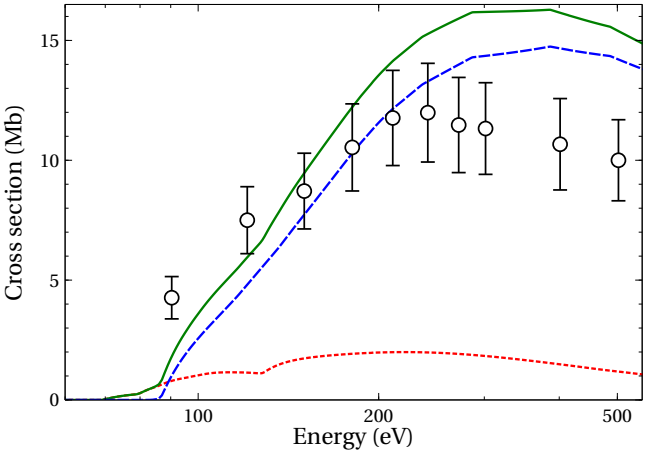

FIG. 6. Electron-impact DI of Se^{2+}. Dotted line (red): DDI cross sections when one of the electrons takes all excess energy; dashed line (blue): indirect DI cross sections; solid line (green): total DI cross sections; empty circles: experiment [13].

$4s\,4p^2\,4d$ configuration has 17 levels above the ionization threshold out of 56; $4s\,4p^2\,5s$, 5 out of 16; and $4s\,4p^2\,5p$, 26 out of 42. Distribution of population among the excited levels due to electron-impact excitation is quite complex. However, all excited levels of these configurations produced from $4p^2\,{}^1S_0$ ($4p^2_{1.5}(0)0$ in jj coupling scheme) are above the ionization threshold except for one level for the $4s\,4p^2\,5s$ configuration. This is one of the reasons that determines the higher EA cross sections for the $4p^2\,{}^1S_0$ level compared to other levels of the ground configuration.

Electron-impact DI cross sections for the Se^{2+} ion are shown in Fig. 6. As it is mentioned above, DI is studied from the excited $4p^2\,{}^1S_0$ level. However, the similar results are observed for other levels of the ground configuration. Cross sections of DDI-AI (II, IEI), which result from the $3d$ direct single ionization are subtracted from the IA values as this contributes to TI. As it can be seen from Fig. 6, the main contribution to the total DI cross sections comes from indirect DI process: CI from the $3d$ shell with subsequent autoionization. The contribution from the direct process consists of about 10%.

Total DI cross sections are in a good agreement with experimental values at the energies near the peak of the experimental cross sections. At the lower energies, theoretical cross sections underestimate the experimental results. What is more, the theoretical cross sections strongly overestimate experimental ones at the energies beyond the peak. Such discrepancies correspond to those obtained using the CADW method [18]. We also studied influence of correlation effects on the cross sections of the DI process. The admixed configurations having the largest influence to the ground ones of the Se^{2+} and Se^{3+} ions and Se^{3+} $3d^9 4s^2 4p^2$ configuration are selected using configuration interaction strength (CIS) [29,30]. Previously, CIS has been successfully applied for the investigation of energy levels [31], Auger cascades [24–26], electric dipole [32], and magnetic dipole [33,34] transitions. Unfortunately, the correlation effects do not show significant contribution to the cross sections of the DI process even for the extended bases of interacting configurations. Thus, the reason of disagreement between the theoretical and experimental values is still unclear.

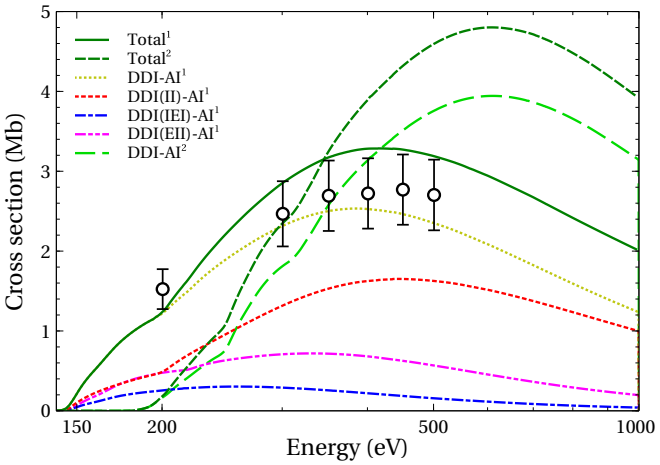

FIG. 7. Contribution of various pathways to the electron-impact TI of Se^{2+}. Superscript 1: TI cross sections when one of the electrons takes all excess energy in the DDI process; superscript 2: TI cross sections when scattered and ejected electrons share the excess energy equally in the DDI process; empty circles: experiment [13]. See explanations in the text for the DDI-AI, DDI(II)-AI, DDI(IEI)-AI, and DDI(EII)-AI processes.

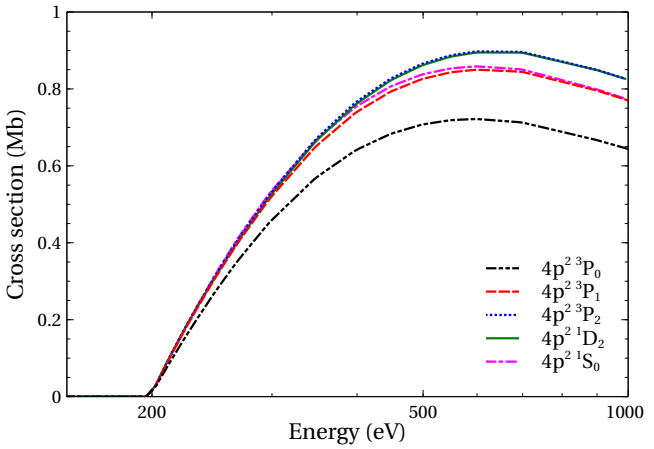

FIG. 8. Electron-impact SI of $3p$ shell of Se^{2+} for energy levels of the ground configuration.

Electron-impact TI cross sections for the Se^{2+} ion are presented in Fig. 7. Here, TI is again investigated from the highest $4p^2\ ^1S_0$ level of the ground configuration. Contribution from the DDI-AI process and Auger cascade following the $3p$ shell ionization is taken into account in the study of the TI process. Theoretical values at the peak are slightly above the experimental data when one of the electrons takes all the excess energy during DDI. It has to be noted that studies that include correlation effects for Auger cascades yield to the ions in the higher ionization stages [25,26]. Thus, one could expect to obtain a better agreement for the TI cross sections. On the other hand, calculations in the potential of the ionized ion provide the cross sections lower by about 20% at the peak. The obtained TI cross sections underestimate experimental ones at the lower energies and overestimate them at the higher energies of the incident electron when the electrons equally share the excess energy.

The largest contribution to the total TI cross sections comes from the DDI-AI process accounting for more than 75% of the total TI cross sections at the peak (Fig. 7). Interestingly, the DDI(II)-AI process contributes to about 70% of the total DDI-AI cross sections and contributions from DDI(II)-AI and DDI(IEI)-AI are smaller. It has to be noted that the two-step II process demonstrates the largest influence to the TI process at the peak. However, three-step processes provide the largest contribution compared to the two-step one at the lower energies of the incident electron. Furthermore, the three-step EII process dominates over the IEI process. This can be explained by the fact that $4s \rightarrow 4p$ and $4p \rightarrow 4d$ excitations have the larger cross sections compared to the ones of ionization from the $3d$, $4s$, and $4p$ shells. What is more, DDI with subsequent Auger cascade also shows contribution to the Se^{6+} ion. However, the cross sections of quadrupole ionization are about an order of magnitude smaller compared to the TI ones.

Configurations of the Se^{4+} ion obtained from DDI for the $4p^2\ ^1S_0$ level and which can decay to Se^{5+} are $3d^8 4s^2 4p^2$, $3d^8 4s\ 4p^3$, $3d^9 4s\ 4p^2$, $3d^9 4p^3$, $3d^9 4s\ 4p\ 4d$, and $3d^9 4s^2 4d$. The highest population is obtained for levels of the $3d^8 4s^2 4p^2$ and $3d^9 4s\ 4p^2$ configurations of Se^{4+} at the peak of the TI cross sections. The third highest population belongs to the $3d^8 4s\ 4p^3$ configuration but its level population is more than a factor of four smaller compared to the first ones. DDI-AI leads to the formation of the Se^{5+} $3d^{10}4s$, $3d^{10}4p$, $3d^{10}4d$, $3d^9 4p^2$, $3d^9 4s^2$, and $3d^9 4s\ 4p$ configurations. The largest population corresponds to the $3d^{10}4s$ and $3d^9 4s\ 4p$ configurations at the peak of the TI cross sections. The population of the other Se^{5+} configurations is about by a factor of two smaller.

Contribution of Auger cascade following SI of $3p$ electron of the Se^{2+} ion accounts for about 25% of the total TI cross sections. The Se^{3+} $3p^5 3d^{10} 4s^2 4p^2$ configuration decays to the Se^{5+} ion through $3d^8 4s^2 4p^2$ and $3d^9 4s^1 4p^2$ configurations. The main path of the population transfer to Se^{5+} goes through $3d^9 4s^1 4p^2$ configuration, especially, at the lower energies of the incident electron.

Ionization of the $3s$ and deeper shells with subsequent Auger cascade has not been analyzed as their SI cross sections are much lower than the ones for the $3p$ shell. Energy levels of configurations produced by ionization of $3d$ shell are below the TI threshold and, thus, this process does not affect the population of the Se^{5+} ions via Auger cascade.

It can also be seen that the excited $4p^2\ ^1S_0$ level for SI of the $3p$ electron of the Se^{2+} ion (Fig. 8) shows significant increase of cross sections over the entire range of energies compared to the contribution of the ground $4p^2\ ^3P_0$ level.

IV. CONCLUSIONS

In this paper, the electron-impact single-, double-, and triple-ionization study is presented for the Se^{2+} ion analyzing transitions among the levels. It is demonstrated that the main part of ions in the parent beam exists in the excited $4p^2\ ^1S_0$ level of the ground configuration. A good agreement between our calculations and experimental measurements is found for the SI of the Se^{2+} ion across the entire energy range of incident

electron with the largest contribution coming from the EA process.

For DI of the Se^{2+} ion, a good agreement with experiment is obtained at the energies near the peak of experimental cross sections. The theoretical cross sections overestimate experimental ones at the higher energies of the incident electron while at the lower energies experimental values are underestimated. The reason of the differences is still unclear. Future experiments could help to resolve this problem.

Current results demonstrate that the TI process is formed by DDI with subsequent autoionization as well as Auger cascade following electron-impact ionization from the $3p$ shell. It is also shown that the knock-out model with subsequent autoionization dominates over the Auger cascade. Furthermore, this suggests that contribution from the direct TI process is very small. A very good agreement with experimental cross sections is found for the TI of the Se^{2+} ion, under assumption that one of the electrons takes all excess energy after the first interaction with the target ion during DDI. The DDI-AI process accounts for more than 75% of the total TI cross sections.

ACKNOWLEDGMENTS

Part of the computations were performed on resources at the High Performance Computing Center HPC Saulėtekis in Vilnius University Faculty of Physics.

[1] K. Bartschat and M. J. Kushner, in *Proceedings of the National Academy of Sciences of the United States of America, Cambridge*, edited by D. A. Weitz (Harvard University, Cambridge, 2016), p. 7026.
[2] R. K. Smith and N. S. Brickhouse, *Advances In Atomic, Molecular, and Optical Physics*, (Academic Press, New York, 2014), Vol. 63, p. 474.
[3] M. Hahn and D. W. Savin, Astrophys. J. **800**, 68 (2015).
[4] J. Bernier, E. J. Hall, and A. Giaccia, Nat. Rev. Cancer **4**, 737 (2004).
[5] Y. Zheng, D. J. Hunting, P. Ayotte, and L. Sanche, Phys. Rev. Lett. **100**, 198101 (2008).
[6] O. Rigaud, N. O. Fortunel, P. Vaigot, E. Cadio, M. T. Martin, O. Lundh, J. Faure, C. Rechatin, V. Malka, and Y. A. Gauduel, Cell Death Dis. **1**, e73 (2010).
[7] I. U. Roederer, H. Schatz, J. E. Lawler, T. C. Beers, J. J. Cowan, A. Frebel, I. I. Ivans, Ch. Sneden, and J. S. Sobeck, Astrophys. J. **791**, 32 (2014).
[8] A. L. Mashburn, N. C. Sterling, S. Madonna, H. L. Dinerstein, I. U. Roederer, and T. R. Geballe, Astrophys. J. **831**, L3 (2016).
[9] N. C. Sterling, S. Madonna, K. Butler, J. Garcia-Rojas, A. L. Mashburn, C. Morisset, V. Luridiana, and I. U. Roederer, Astrophys. J. **840**, 80 (2017).
[10] B. Sharpee, Y. Zhang, R. Williams, E. Pellegrini, K. Cavagnolo, J. A. Baldwin, M. Phillips, and X.-W. Liu, Astrophys. J. **659**, 1265 (2007).
[11] N. C. Sterling and M. C. Witthoeft, Astron. Astrophys. **529**, A147 (2011).
[12] I. U. Roederer, Astrophys. J. **756**, 36 (2012).
[13] G. A. Alna'washi, N. B. Aryal, K. K. Baral, C. M. Thomas, and R. A. Phaneuf, J. Phys. B **47**, 135203 (2014).
[14] G. A. Alna'washi, K. K. Baral, N. B. Aryal, C. M. Thomas, and R. A. Phaneuf, J. Phys. B **47**, 105201 (2014).
[15] R. Rejoub and R. A. Phaneuf, Phys. Rev. A **61**, 032706 (2000).
[16] W. Lotz, Z. Phys. **216**, 241 (1968).
[17] V. P. Shevelko, H. Tawara, I. Yu. Tolstikhina, F. Scheuermann, B. Fabian, A. Müller, and E. Salzborn, J. Phys. B **39**, 1499 (2006).
[18] M. S. Pindzola and S. D. Loch, J. Phys. B **49**, 125202 (2016).
[19] V. Jonauskas, A. Prancikevičius, Š. Masys, and A. Kynienė, Phys. Rev. A **89**, 052714 (2014).
[20] J. Koncevičiūtė and V. Jonauskas, Phys. Rev. A **93**, 022711 (2016).
[21] G. Purohit, P. Singh, A. Dorn, X. Ren, and V. Patidar, J. Electron Spectrosc. Relat. Phenom. **209**, 40 (2016).
[22] M. J. Ambrosio, D. M. Mitnik, A. Dorn, L. U. Ancarani, and G. Gasaneo, Phys. Rev. A **93**, 032705 (2016).
[23] V. Jonauskas, L. Partanen, S. Kučas, R. Karazija, M. Huttula, S. Aksela, and H. Aksela, J. Phys. B **36**, 4403 (2003).
[24] V. Jonauskas, R. Karazija, and S. Kučas, J. Phys. B **41**, 215005 (2008).
[25] J. Palaudoux, P. Lablanquie, L. Andric, K. Ito, E. Shigemasa, J. H. D. Eland, V. Jonauskas, S. Kučas, R. Karazija, and F. Penent, Phys. Rev. A **82**, 043419 (2010).
[26] V. Jonauskas, S. Kučas, and R. Karazija, Phys. Rev. A **84**, 053415 (2011).
[27] M. F. Gu, Can. J. Phys. **86**, 675 (2008).
[28] A. Kramida, Yu. Ralchenko, J. Reader, and and NIST ASD Team, NIST Atomic Spectra Database (ver. 5.1), 2013.
[29] R. Karazija, *Introduction to the Theory of X-Ray and Electronic Spectra of Free Atoms* (Plenum Press, New York, 1996).
[30] S. Kučas, V. Jonauskas, and R. Karazija, Phys. Scr. **55**, 667 (1997).
[31] L. Radžiūtė, G. Gaigalas, D. Kato, P. Jönsson, P. Rynkun, S. Kučas, V. Jonauskas, and R. Matulianec, J. Quant. Spectros. Radiat. Transfer **152**, 94 (2015).
[32] A. Kynienė, S. Kučas, V. Jonauskas, and R. Karazija, Lith. J. Phys. **48**, 219 (2008).
[33] V. Jonauskas, R. Kisielius, A. Kynienė, S. Kučas, and P. H. Norrington, Phys. Rev. A **81**, 012506 (2010).
[34] V. Jonauskas, G. Gaigalas, and S. Kučas, At. Data Nucl. Data Tables **98**, 19 (2012).